



## Reduction of $\text{Cu}^{+2}$ and $\text{Ni}^{+2}$ Ions from Wastewater Using Mesoporous Adsorbent: Effect of Treated Wastewater on Corrosion Behavior of Steel Pipelines



M. F. Shehata<sup>1</sup>, Shaymaa E. El-Shafey<sup>2</sup>, Nabila S. Ammar<sup>3</sup>, A. M. El-Shamy<sup>1</sup>

<sup>1</sup>Physical Chemistry Department, Electrochemistry and Corrosion Lab., National Research Centre, El-Bohouth St. 33, Dokki, P.O. 12622, Giza, Egypt.

<sup>2</sup>Physical Chemistry Department, Surface Chemistry and Catalysis Lab., National Research Center, El-Bohouth St. 33, Dokki, P.O. 12622, Giza, Egypt.

<sup>3</sup>Water Pollution Research Department, National Research Centre, El-Bohouth St. 33, Dokki, P.O. 12622, Giza, Egypt.

**L**ARGE amounts of highly heavy metals contaminated wastewater effluents are produced through the metal finishing and electroplating processes. In this study, mesoporous zeolite was prepared from Egyptian bentonite by alkali-hydrothermal method. The prepared zeolite was characterized by XRD technique showing the formation of crystalline phases corresponded to the zeolite structure. The adsorption performance of zeolite toward removal of copper ( $\text{Cu}^{+2}$ ) and nickel ( $\text{Ni}^{+2}$ ) ions was studied in relation to effect of contact time, concentrations of metal ions and the dose of adsorbent. The effect of  $\text{Cu}^{+2}$  and  $\text{Ni}^{+2}$  ions in treated wastewater on the corrosion behavior of steel pipelines was demonstrated. Elovich, Pseudo-first-order and Pseudo-second order kinetic models were applied. Kinetics models revealed that the adsorption of both  $\text{Cu}^{+2}$  and  $\text{Ni}^{+2}$  on zeolite was controlled by pseudo-second order kinetic and the equilibrium achieved at 90 min. Langmuir, Freundlich and Dubinin–Kaganer–Radushkevich isotherms were investigated and the results showed that the adsorption of both cations well-satisfied with Langmuir model. The free energy (E) was 10.66 and 8.772 kJ/mol for the adsorption of  $\text{Cu}^{+2}$  and  $\text{Ni}^{+2}$  ions, respectively, confirming that the adsorption mechanism is endothermic and proceed through ion-exchange. The effect of  $\text{Cu}^{+2}$  and  $\text{Ni}^{+2}$  on the corrosion behavior of steel pipelines revealed that the corrosion resistance of steel for treated and untreated water is almost the same.

**Keywords:** Zeolite, Copper and Nickel, Isotherm, kinetics, Corrosion.

### Introduction

Discharging of metal cations into water streams is considered the key cause of soil water pollution. These cations have an affinity to collect in the organisms and cause several diseases [1-3]. The heavy metals can be removed by using many techniques such as; ultra-filtration, precipitation, phyto-extraction, reverse osmosis (RO), and electro-dialysis (ED). All of these techniques have abundant ability for removing metal ions and organometallic wastes from industrial effluents [4-6]. These techniques are expensive, so low-cost adsorbent materials are considered as alternative

potential applicable technique for removing cations from industrialized wastewater. An ion exchange processes measured as cost effective techniques if zeolites are applied [7-9]. Zeolites are naturally occurring tectosilicates and there are three dimensional complexes of aluminate and silicone dioxide tetrahedral connected by joint venture of each and every one oxygen atom. In addition, zeolites contain several cations replaceable with other positive ions in the effluents [10-12]. Many researchers showed high interest to investigate the adsorption performance of zeolite in removing metal ions from wastewater based on its exceptional distinctive sorts as adsorption and ion

\*Corresponding author e-mail: s\_shafey@yahoo.com

Received 5/2/2019; Accepted 19/3/2019

DOI:10.21608/ejchem.2019.7967.1627

©2019 National Information and Documentation Center (NIDOC)

exchangeable techniques [13]. As accomplished from previous work, this adsorbent has been engaged to uptake many cations from artificial solutions. The main task of this study is focused on examining the capacity of zeolite for removing  $\text{Cu}^{+2}$  and  $\text{Ni}^{+2}$  ions using the kinetic and adsorption isotherm models.

Appreciative understanding of the corrosion and corrosion control in treated and untreated wastewater necessitate good awareness of the surrounding environment since whether it corrosive or non-corrosive [14]. Primarily the engineering process of wastewater management depends on handling some of the existing corrosive and aggressive materials. All steel structures suffer from corrosion due to existence of many limitations as chemical compounds, industrial wastes, corrosive chemicals and corrosive gases. The steel pipe and the tank of wastewater handling plant are generally damaged by microbial corrosion [15, 16]. Biological treatments of wastes depend on cultivation of bacteria and/or other microorganisms at their extreme growth rate, so the corrosion process is observed. Chlorine and ozone are applied as cleansing agents in the final step of treatment, which add extra corrosion factors. Not only the microorganisms which influence the deterioration of the pipelines and tanks but also many extra reasons such as, organic compounds including fats, greases, proteins, surfactants, oils, pesticides and phenols affect them. The corrosive vapors such as  $\text{H}_2\text{S}$ ,  $\text{CH}_4$ ,  $\text{NH}_3$ ,  $\text{O}_2$ ,  $\text{CO}_2$  and  $\text{N}_2$  are usually dissolved in industrial wastewater. The heavy metals are considered the supreme energetic and toxic in petroleum and electroplating industry [17]. However, the attendance of cations is getting benefits for corrosion defense of pipelines. Its exact significant is to remove heavy metals owing to its toxicity. For solving the corrosion problem the sedimentation tanks are constructed of concrete, so our work is focused on the pipeline protection against corrosion after passing the treatment process.

## Materials and Methods

### Raw materials

Bentonite clay occurs in several zones in Egypt and utilized in different purposes. Clay contents and its behavior were inspected in relation to steel corrosion. The bulk samples of bentonite were acquired from Al-Alamine area. The bentonite is crushed, milled and distributed over 300X600- $\mu\text{m}$  mesh and then dehydrated in a heater at  $100 \pm 5^\circ\text{C}$  for 1 day.

### Zeolitization process

Zeolitization of the natural alumina-silicate bentonite was supported by admixing 1g of the raw material with 3M of NaOH solution in tightly closed Teflon tube under stirring for about 12 hours till whole

dissolution. Then, it was transferred into a stainless steel reactor and put in an air oven at  $80^\circ\text{C}$  for an aging period of 1 week. After the crystallization, the product (reaction gel) was centrifuged and washed for several times till  $\text{pH} = 7$  and dried at  $65^\circ\text{C}$ .

### Characterization tools

The crystalline phases for the investigated sample were determined by x-ray diffraction analysis using a Bruker diffractometer (Bruker D8 advance, Germany). The patterns were run with CuK $\alpha$ 1 target with secondly monochromator 40 kV, 40 mA. The surface structure and the energy-dispersive X-ray spectroscopy (EDX) measurements of the prepared sample was estimated by field-emission scanning electron microscope (SEM) (FE-SEM, FEI Quanta FEG-250).

### Reagents

The chemicals were provided from Merck in a highly purified grade. The reagents were prepared by using de-ionized water. Stock solutions of  $\text{Cu}^{+2}$  and  $\text{Ni}^{+2}$  were prepared in deionized and/or double distilled water from ( $\text{CuSO}_4 \cdot 5\text{H}_2\text{O}$ ) (Merck) and [ $\text{Ni}(\text{Cl})_2 \cdot 6\text{H}_2\text{O}$ ], correspondingly.

### Batch adsorption experiments

The adsorption experiments in batch mode were applied to test the different factors affecting on the adsorption procedure as contact time, metal ions concentrations and dose of adsorbent. The experiments were implemented by stirring certain adsorbent dose in 100 mL of the synthetic contaminated solutions at pH of 5 and at  $25^\circ\text{C}$  in 150mL plastic flasks. The treated trials were spelled out using filter paper (Whatman No. 42). The metal concentrations were determined by using plasma spectrometry (Agilent ICP-OES 5100, Australia) [18]. All tests were reiterated three times and the removal percentage of metal ions by zeolite was determined using the subsequent formula 1:

$$\text{Adsorption, \%} = \frac{(C_i - C_f)}{C_f} \times 100 \quad (1)$$

Where  $C_i$  and are the initial and final concentrations (mg/L) of the metal ions solutions, respectively.

$$K_d = \frac{\text{amount of metal in adsorbent}}{\text{amount of metal in solution}} \times \frac{V}{m} \quad (2)$$

Where  $V$  is the volume of the solution (ml) and  $m$  is the weight of the adsorbent (g).

### Corrosion Monitoring

#### Electrochemical techniques

The test electrodes were set from mild steel sample as working electrode. The electrode was fixed in a resin from araldite epoxy in a Pyrex tube parting space

of the electrode of about  $0.75 \text{ cm}^2$ . Earlier for each test the surface was polished continually using different grades of emery papers to 1500 grit, cleaned alongside by soft refining cloth. The greased surface was re-cleaned by acetone prior test. The cell comprised of an emblematic 3 electrodes. A saturated calomel electrode (SCE) was used as the reference electrode and platinum sheet of size  $15 \text{ mm} \times 20 \text{ mm} \times 2 \text{ mm}$  as the auxiliary electrode. Polarization experiments were verified at  $1 \text{ mV s}^{-1}$  scan rate after parting 30 min to acquire a steady state potential [19, 20].

## Results and Discussion

### Zeolite characterization

To a sample of zeolite powder is categorized by XRD technique before treatment and the data are contemporary in Fig. 1. The XRD patterns confirm the formation of crystalline phases corresponded to the zeolite structure [21]. EDX analysis in Fig. 2 revealed the presence of Si, Al, Na, Mg and Ca elements as well as and their chemical compositions are shown in Table 1.

The ratio between silicon and aluminum is typically with clinoptilolite and this ratio is agreed with Galli [22]. The sodium and potassium oxides were analyzed by flame photometry. In addition, as seen in Table 1, the Chabazite is considered as zeolite family and based on its modes of occurrence and internal structures [21, 23]. The cation-exchange properties are brought from the being of Al atoms instead of Si atoms, which creates the negative charge sites on the surface of zeolite. These properties are very important in exclusion of cations and in water softeners due to exchange of cations as  $\text{Na}^+$ ,  $\text{Mg}^{2+}$  and  $\text{Ca}^{2+}$ . Moreover, SEM image illustrates the formation of layers with cavities on the surface of zeolite.

### Influence of contact time

It is essential to test the best time of zeolite and contaminated solution with metal ions [24]. The experiment was considered by means of  $20 \text{ mg/L}$  as of individually  $1.0 \text{ gm/L}$  of metal ion with zeolite at time recesses (5, 15, 30, 60, 90 and 120 min) and at temp  $25^\circ \text{C}$ . Figure 3 showed that removal process of both  $\text{Cu}^{+2}$  and  $\text{Ni}^{+2}$  proceeded quickly until 90 min. The removal efficiency at this time was 84%. Noticeably seen that

in the 90 min the uptake capability reached about  $15.7 \text{ mg/g}$  (84%) and  $16.8 \text{ mg/g}$  (78.5%) for  $\text{Cu}^{+2}$  and  $\text{Ni}^{+2}$  ions, respectively.

At 120 min, the capacities of zeolite adsorbent were nearby to that at 90 min and thus the adsorption balance was achieved at 90 min.

### Influence of adsorbent dose

Different zeolite doses ranging from  $0.5\text{--}5.0 \text{ g/L}$  were used to test the adsorption capability of adsorbent dose at the optimum contact time and at  $25^\circ \text{C}$ . Figure 4 showed that the removal efficiency of  $\text{Cu}^{+2}$  (66.75- 84.5%) and  $\text{Ni}^{+2}$  (51-81.5%) enlarged increasing of adsorbent dose because of the greater surface area ( $500\text{--}800 \text{ m}^2/\text{g}$ ) [25]. In case of  $0.2 \text{ g}$  dose, the increase of  $\text{Cu}^{+2}$  and  $\text{Ni}^{+2}$  removal is marginally. In this situation there is an equilibrium between the metal concentration and the number of uptake spots [26]. Therefore, it was considered that the optimum adsorbent dose for both  $\text{Cu}^{+2}$  [84% ( $16.8 \text{ mg/g}$ )] and  $\text{Ni}^{+2}$  [79% ( $15.7 \text{ mg/g}$ )] was achieved at  $2 \text{ g/L}$  of zeolite.

### Influence of initial metal ions concentration

This study was identified at the optimum conditions of contact time (90 min), zeolite dose ( $2 \text{ g/L}$ ), pH of 5 and  $25^\circ \text{C}$ . The studied initial concentrations of  $\text{Cu}^{+2}$  and  $\text{Ni}^{+2}$  were [20, 40, 80 and  $120 \text{ mg/L}$ ]. As revealed in Fig. 5, the adsorption capacity is in direct relation with metal concentration. The rise of adsorption capacity is affected by the metal ions concentration till specific value even further increase in metal ions concentration [27- 29]. Therefore, Langmuir, Freundlich and Dubinin–Kaganer–Radushkevich (DKR) models are necessary for studying the adsorption mechanism as showed in the following section [30].

### Isotherm Models

Langmuir, Freundlich and Dubinin–Kaganer–Radushkevich isotherms are applied to determine the maximum capacity. Langmuir isotherm assumes that the adsorption discriminate a formation of one layer onto the active surface. This phenomenon could be proved from the simplified linear form as in the following equation [30, 31]:

**TABLE 1. The mineralogical analysis of zeolite sample before adsorption experiment.**

Ref. Code	Mineral Name	Chemical Formula
01-084-0698	Clinoptilolite	$\text{Na}_3.68(\text{Al}_3.6\text{Si}_8.4\text{O}_{24})(\text{H}_2\text{O})1.2$
00-044-0248	Chabazite-Na, syn	$\text{NaAlSiO}_4 \cdot x\text{H}_2\text{O}$
00-020-0452	Gismondine	$\text{CaAl}_2\text{Si}_2\text{O}_8 \cdot 4\text{H}_2\text{O}$

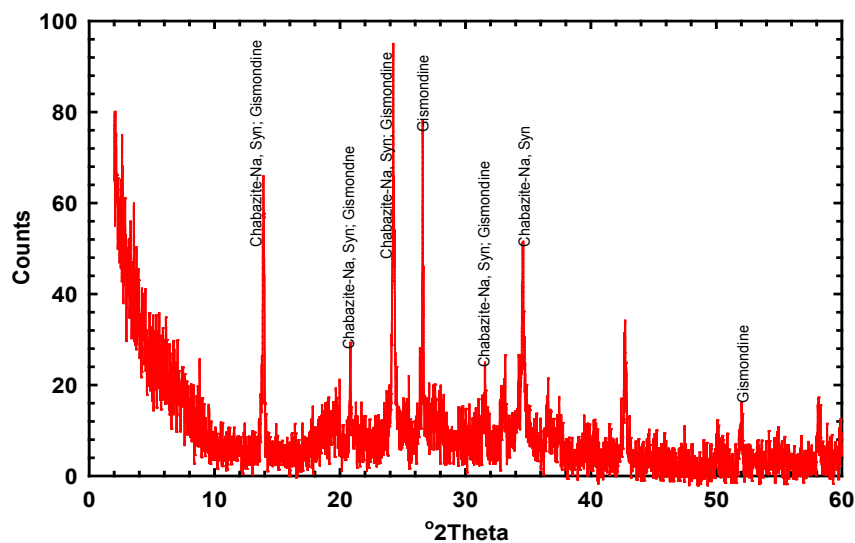


Fig. 1. XRD patterns for the powder of zeolite sample.

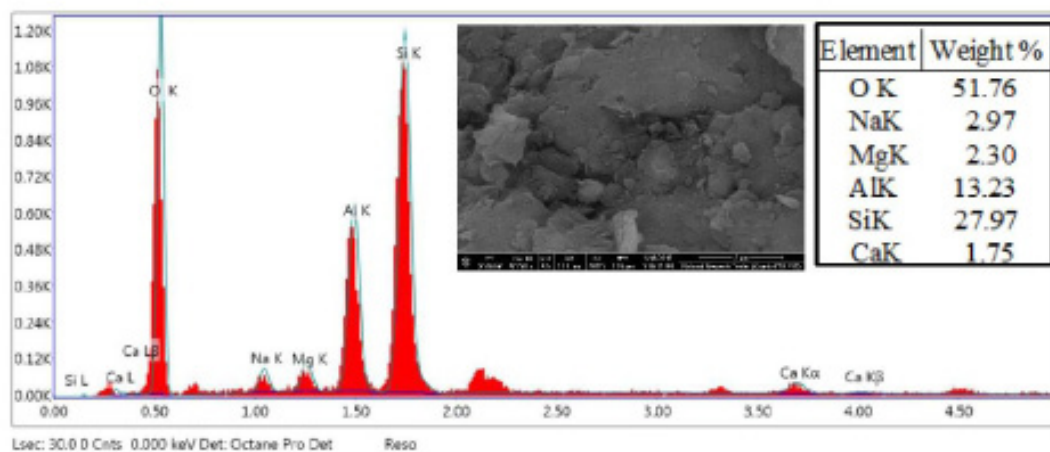


Fig. 2. EDS and SEM images of the obtained zeolite sample.

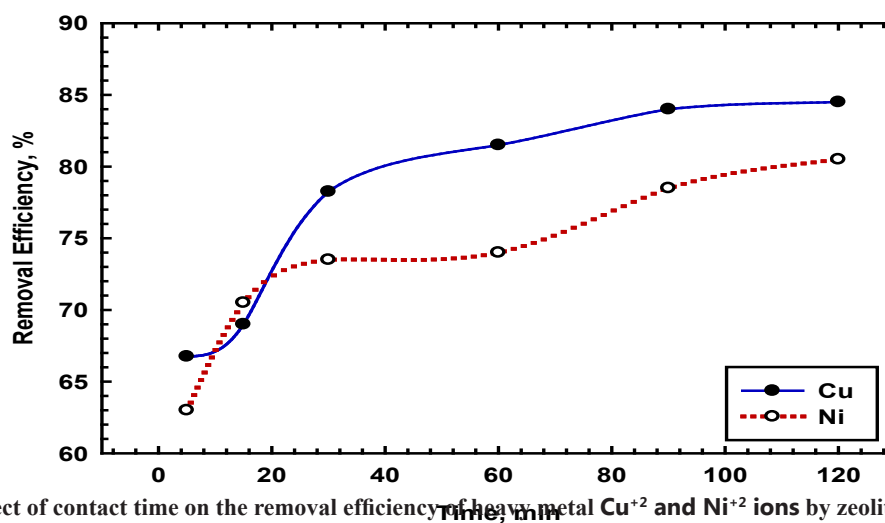


Fig. 3. Effect of contact time on the removal efficiency of heavy metal  $\text{Cu}^{+2}$  and  $\text{Ni}^{+2}$  ions by zeolite:  $C_i = 20$  mg/L,  $V = 100$  mL,  $\text{pH} = 5$ ,  $T = 25^\circ\text{C}$  and adsorbent dose =  $0.1$  g.

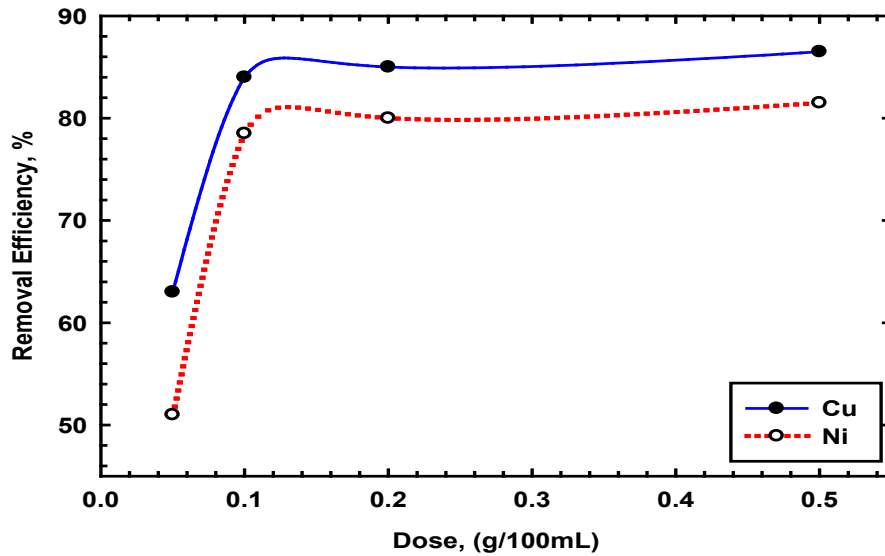


Fig. 4. Effect of adsorbent dose on the removal efficiency of  $\text{Cu}^{+2}$  and  $\text{Ni}^{+2}$  ions by zeolite:  $C_i = 20 \text{ mg/L}$ ,  $V = 100 \text{ mL}$ ,  $\text{pH} = 5$ ,  $\text{time} = 90 \text{ min}$  and  $T = 25^\circ \text{C}$ .

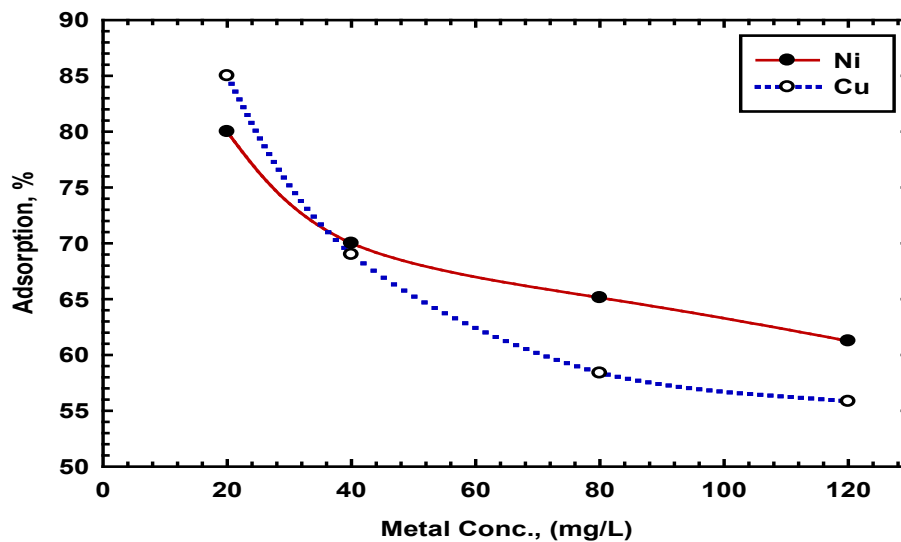


Fig. 5. Effect of initial concentration of heavy metals on the removal efficiency of  $\text{Cu}^{+2}$  and  $\text{Ni}^{+2}$  ions:  $C_i = 20 \text{ mg/L}$ ,  $V = 100 \text{ mL}$ ,  $\text{pH} = 5$ ,  $\text{time} = 90 \text{ min}$  and  $T = 25^\circ \text{C}$

$$\frac{C_e}{q_e} = \frac{1}{Qb} + \frac{C_e}{Q} \quad (4)$$

$C_e$  initial concentration of metal ions in solution (mg/L),

$q_e$  number of adsorbed metal ions onto the adsorbent (mg/g),

$b$  the equilibrium adsorption constant which is related to the affinity of the binding sites (L/g)

$Q$  the maximum amount of metal ion per unit mass of sorbent when all binding sites are occupied (mg/g)

By plotting  $C_e/q_e$  vs.  $C_e$ , the rationality of the Langmuir giving  $R^2$  value nearby to unity since, the  $Q$  and  $b$  are gained from lined progression of Langmuir isotherm as shown in Fig. 6b, 7b for  $Ni^{+2}$  and  $Cu^{+2}$  ions sorption correspondingly. The zeolite is generally act as weak acid so sodium form replacers is highly selective for hydrogen ions, then high pH is obtained at equilibrium with dilute solutions, which precipitate the  $M^{++} (OH)^-$ . In this case the zeolite appears to touch the full capacity, which means that the ions had occupied the probable presented sites. The further adsorption process could be realized by existing new unoccupied sited through existing an original surface. Generally, the cations exist in complexes with six water particles and distributed from side to side of zeolite channels [32]. It is well acknowledged that, the elimination process being contingent with the attentiveness of charge and the hydrated cations diameter.

The Freundlich equation is given by:

$$\log q_e = \log K_f + \frac{\log c_e}{n} \quad (5)$$

$C_e$  the equilibrium concentration in (mg/L),  
 $K_f$  Freundlich constants and are related to the adsorption capacity of the sorbent  
 $n$   $(mg/g)/(L/mg)^{1/n}$   
 adsorption intensity

The value of  $n$  (the heterogeneity factor) describes the nature of adsorption process where if  $n = 1$ , it is linear, if  $n > 1$ , it is a physical process favorable, and if  $n < 1$ , it is a chemical process. This model has generally defined the adsorption features on the dissimilar surface [33]. The values of  $K_f$ , and  $n$  are cached from investigational results by linear regression as publicized in Fig. 6a, 7a for  $Ni^{+2}$  and  $Cu^{+2}$  ions sorption respectively. The isotherms of Langmuir and Freundlich are mostly depending on the equilibrium data see Tables 2 and 3.

**TABLE 2. Langmuir parameters of the  $Cu^{+2}$  and  $Ni^{+2}$  adsorbed by zeolite.**

Metal	$Q$ (mg/g)	$b$ (L/g)	$R^2$
$Cu^{2+}$	43.5	0.029	0.8907
$Ni^{2+}$	62.5	0.049	0.9015

**TABLE 3. Freundlich adsorption parameters of the  $Cu^{+2}$  and  $Ni^{+2}$  adsorbed by zeolite.**

Metal	$K_f$ (mg/g)/(L/mg) <sup>1/n</sup>	$n$	$R^2$
$Cu^{2+}$	4.76	2.15	0.973
$Ni^{2+}$	4.43	1.60	0.992

The values of  $R^2$  for  $Cu^{+2}$  and  $Ni^{+2}$  are 0.8907 and 0.9015, respectively. Since it is exposed that enormously bad application of Langmuir model. The values of  $R^2$  in the second model was  $>0.97$  for both  $Cu^{+2}$  and  $Ni^{+2}$  ions, this indicating that Freundlich isotherm only was adequately describing the investigational data of  $Cu^{+2}$

and  $Ni^{+2}$  ions which it does not accept a homogeneous surface, so it is extensive model as associated to Langmuir.

The linear formula of DKR isotherm can be streamlined as publicized in Eq(6):

$$\ln C_{ads} = \ln X_m - \beta \varepsilon^2 \quad (6)$$

$C_{ads}$  the number of adsorbed metal ions per adsorbent weight unity (mol/g),  
 $X_m$  the extreme capacity of adsorption (mmol/kg) [34],  
 $\beta$  the coefficient associated to the energy of adsorption process (mol<sup>2</sup> k/J<sup>2</sup>),  
 $\varepsilon$  the Polanyi potential is spontaneous commencing the subsequent formula:

$$\varepsilon = RT \ln \left( 1 + \frac{1}{C_e} \right) \quad (7)$$

$R$  the general gas constant (kJmol<sup>-1</sup> K<sup>-1</sup>),  
 $T$  the temperature (K).

The adsorption capacity,  $X_m$  (mmol/kg) can be spontaneous from the intercept of plotting the slope of  $\ln C_{\text{ads}}$  versus  $\varepsilon$  and the adsorption energy can be assessed from following equation:

$$E = 1/\sqrt{-2\beta} \quad (8)$$

Figures 6c and 7c represented by plotting  $\ln q_e$  against  $\varepsilon$  for  $\text{Cu}^{2+}$  and  $\text{Ni}^{2+}$  sorption on zeolite and the calculated parameters of DKR model are mentioned

TABLE 4. DKR adsorption equations of  $\text{Cu}^{2+}$  and  $\text{Ni}^{2+}$  ions adsorbed by zeolite.

Metal	$X_m$ (mol/g)	$\beta$ , (mol <sup>2</sup> /j <sup>2</sup> )	E(KJ/mol)	$R^2$
$\text{Cu}^{2+}$	$1.81 \times 10^{-3}$	$-0.44 \times 10^{-8}$	10.7	0.957
$\text{Ni}^{2+}$	$3.93 \times 10^{-3}$	$-0.605 \times 10^{-8}$	8.77	0.984

in Table 4. It displays that, the  $E$  values are 10.66 and 8.772 kJ/mol for  $\text{Cu}^{2+}$  and  $\text{Ni}^{2+}$  correspondingly. These positive values of  $E$  specify that the process is endothermic. Since the sorption energy in DKR equation is between 8-16 kJ/mol representing that the mechanism of process is ion-exchange. The capability  $X_m$  in the DKR is  $1.81 \times 10^{-3}$  for  $\text{Cu}^{2+}$  and  $3.93 \times 10^{-3}$  mmol/kg for  $\text{Ni}^{2+}$  [36].

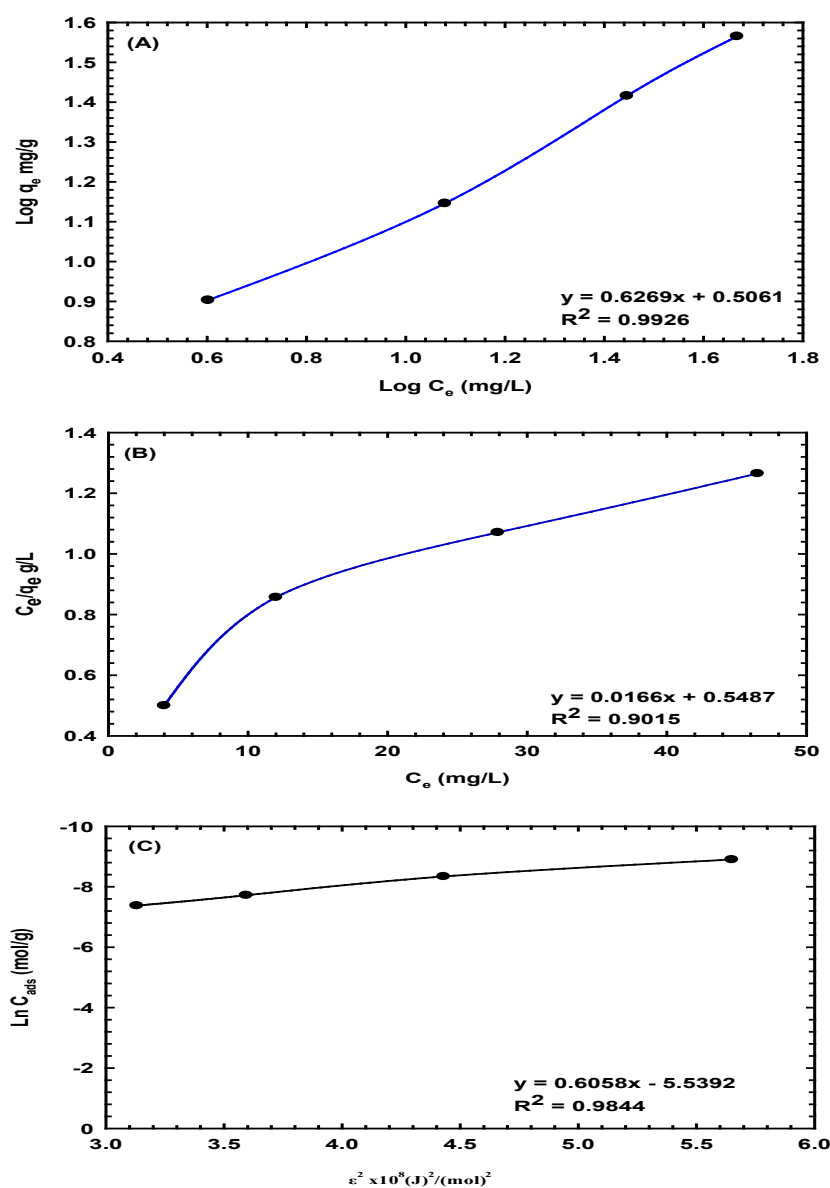


Fig. 6. Adsorption isotherms for  $\text{Ni}^{2+}$  ions onto zeolite (A) Freundlich adsorption isotherm plot (B) Langmuir adsorption isotherm plot (C) Dubinin–Kaganer–Radushkevich (DKR).

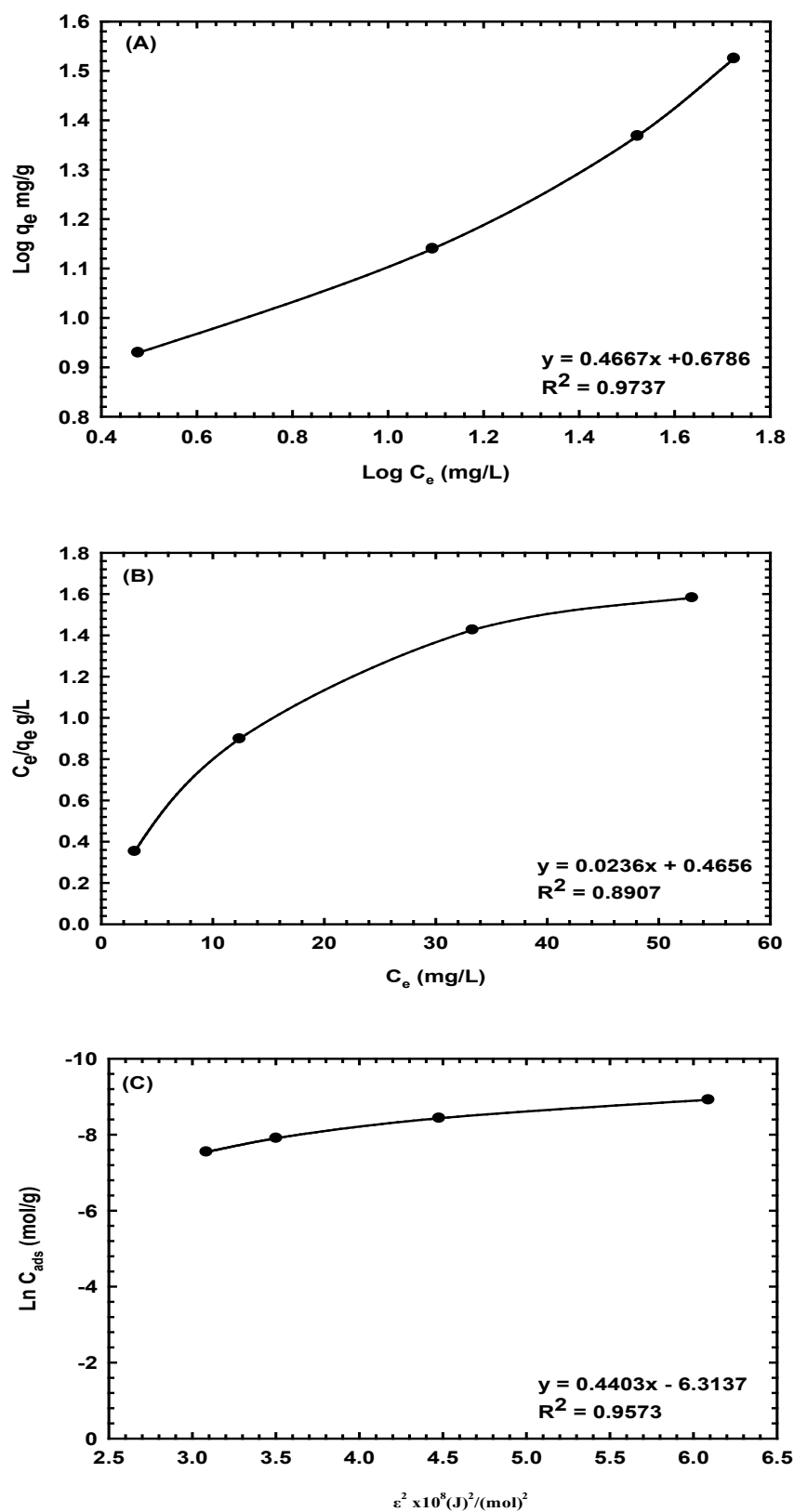


Fig. 7. Adsorption isotherms for  $\text{Cu}^{2+}$  ions onto zeolite (A) Freundlich adsorption isotherm plot, (B) Langmuir adsorption isotherm plot (C) Dubinin-Kaganer-Radushkevich (DKR) isotherm plot.

*Effect of the distribution ratio ( $K_d$ )*

At persistent temperature the ( $K_d$ ) of  $\text{Cu}^{+2}$  and  $\text{Ni}^{+2}$  onto zeolite as a purpose of their concentrations were calculated. The tested concentrations of metal ions are (20, 40, 80 and 120 mg/L at the optimum operating conditions. The ( $K_d$ ) was considered by means of the previous formula 2. Figure 8 illustrates the relation between  $K_d$  and the metal ions concentrations which shows that the  $K_d$  values growth with declining the metal ions concentration [37]. The data show that, the less actively promising spots be intricate with growing the concentration of metal ions. The results show greatest interchange ranks were  $\text{Cu}^{2+}$  (85 %) >  $\text{Ni}^{2+}$  (80

%). The adsorption percentage of cations diminutions with growing of the cations concentration in liquid phase. These results proved that, the purging of cations are accredited to dissimilar appliances of adsorption process and/or ion-exchange process. In case of ion-exchange process, the cations are moving from side to side of the zeolite pores. These cations pass through lattice channels of zeolite and replacing  $\text{Na}^+$  and  $\text{Ca}^{2+}$ . The values of  $K_d$  are enlarged by reduction of cations in electrolyte. The supreme levels of ion interchange are achieved when the efficiencies of cations are  $\text{Cu}^{2+}$  85 % and  $\text{Ni}^{2+}$  80 %.

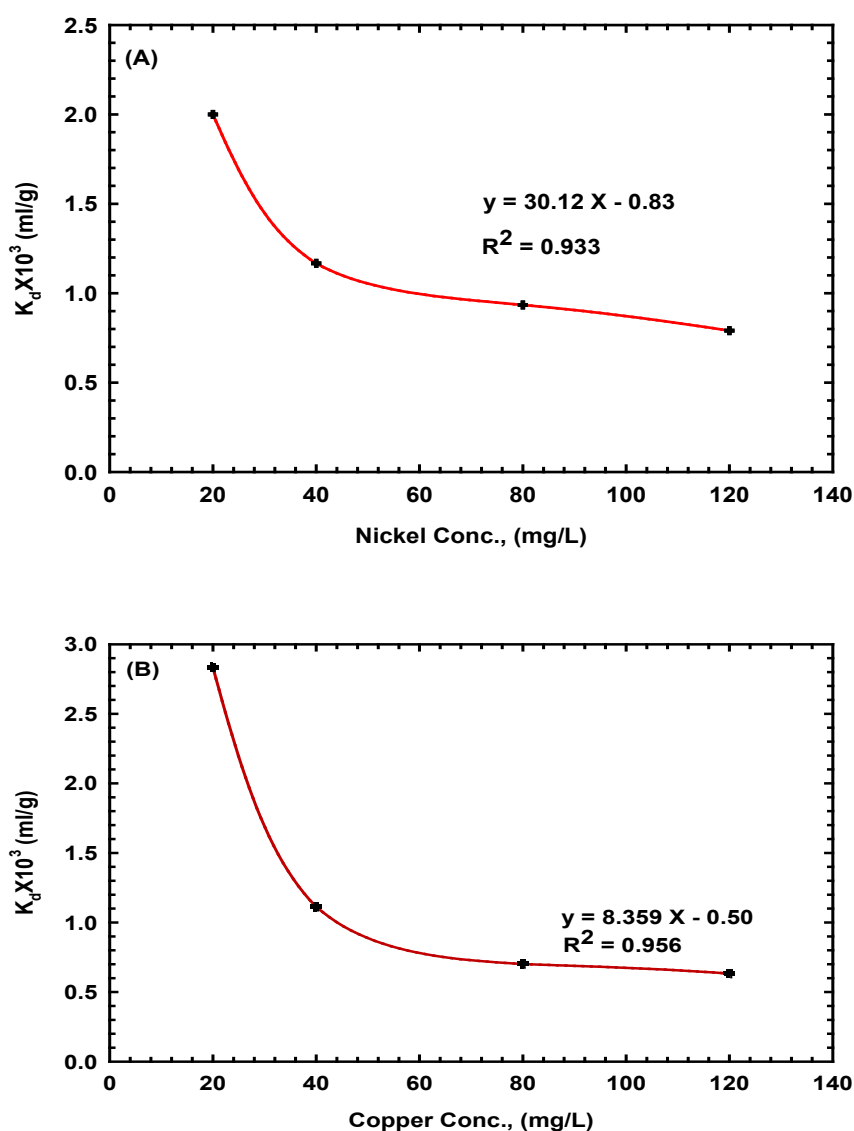


Fig. 8. Variation of distribution coefficients (A)  $\text{Ni}^{+2}$  (B)  $\text{Cu}^{+2}$  ions on zeolite as a function of initial concentrations at the optimum removal conditions.

### The kinetic models

Sorption kinetics of zeolite be governed by the occurrence of active spots, the simplicity of contact of the metal ions on the active spot without sterically hindrance [38]. The adsorption kinetics were studied by applying the commonly replicas as Elovich, pseudo first and second order models. The arrangement between investigational and theoretical models is anticipated by the comparatively developed R<sup>2</sup> values (close to 1).

#### Pseudo first order kinetic model

Pseudo first order kinetic model is articulated by the subsequent lined form as in Eq. 9 [39].

$$\log (q_e - q_t) = \log q_e - k_1 t / 2.303 \quad (9)$$

$q_e$  and  $q_t$  (meq/g)      the amounts of metal ions adsorbed onto the sorbent at equilibrium and at time  $t$   
 $t$  (min)                      the initial rate of adsorption (mg/gmin)  
 $k_1$  (min<sup>-1</sup>)                   $k_1$  (min-1)                  The Lagergren rate constant of the pseudo-first-order.

#### Pseudo second order kinetic model

The kinetics were described by the pseudo second order model [40] as shown in the following Eq. 10:

$$t/q_t = 1/k_2 q_e^2 + t/q_e \quad (10)$$

$k_2$  (g/mg min)      the rate constant of second order adsorption

The slope and intercept were used to calculate  $K_2$  and  $q_e$  by plotting of  $t/q_t$  against  $t$  as shown in Fig. 10 and Table 5 represents the parameters of pseudo-

The slope and intercept provide the values of  $K_1$  and  $q_e$  by plotting  $\log (q_e - q_t)$  against  $t$  (Fig. 9). Table 5 represents the values of pseudo first order parameters and the adsorption constants are 0.062 and 0.005 min<sup>-1</sup>. The values of R<sup>2</sup> are 0.797 and 0.527 for Cu<sup>+2</sup> and Ni<sup>+2</sup> adsorption correspondingly on zeolite. These results indicated that the calculated  $q_e$  [2.19 mg/g for Cu<sup>+2</sup> and 3.39 for Ni<sup>+2</sup>] values don't agree with the experimental  $q_e$  values [0.529 meq/g for Cu<sup>+2</sup> and 0.535 for Ni<sup>+2</sup>] in addition, the values of correlation coefficients (R<sup>2</sup>) are very low. Therefore, it is unfavorable to apply this model for predicting kinetics of metal ions adsorption on zeolite.

second-order of about 0.68 and 0.632 min<sup>-1</sup> and the values of R<sup>2</sup> are 0.999 and 0.998 for Cu<sup>+2</sup> and Ni<sup>+2</sup> adsorption correspondingly. These results indicated that the calculated  $q_e$  [0.543 mg/g for Cu<sup>+2</sup> and 0.554 mg/g for Ni<sup>+2</sup>] values well close to the experimental  $q_e$  values [0.529 meq/g for Cu<sup>+2</sup> and 0.535 for Ni<sup>+2</sup>]. In addition, the values of R<sup>2</sup> are very close to 1. Therefore, this model is suitable for predicting the kinetics of Cu<sup>+2</sup> and Ni<sup>+2</sup> adsorption onto zeolite.

**TABLE 5. Parameters of pseudo-first order and pseudo-second models.**

	Cu <sup>+2</sup>	Ni <sup>+2</sup>
Exp $q_e$	0.529	0.535
<b>Pseudo-first -order kinetic model</b>		
$K_1$	0.062	0.005
$q_e$	2.192	3.39
$R^2$	0.797	0.527
<b>Pseudo-second-order kinetic model</b>		
$K_2$	0.68	0.632
$q_e$	0.543	0.554
$R^2$	0.999	0.998

#### Elovich model

This model established on the capacity of adsorption and could be conveyed in the following formula [41, 42]

$$dq/dt = \alpha \exp(-\beta q) \quad (11)$$

This formula is shortened by supposing  $\alpha\beta t \gg t$  and in case of boundary conditions i.e;  $q_t = 0$  at  $t = 0$  and  $q_t = q_e$  at  $t = t$ , then a new formula become in this form:

$$q_t = 1/\beta \ln(\beta\alpha) = 1/\beta \ln(t) \quad (12)$$

By plotting  $q_t$  versus  $\ln(t)$ , a straight line is obtained with a slope of  $(1/\beta)$  and an intercept of  $(1/\beta) * \ln(\beta\alpha)$  as seen in Fig. 11. The Correlation coefficients obtained by Elovich model (0.957 and 0.944 for nickel and copper respectively) were in between the correlation coefficients of pseudo first and second order model. These confirm that the mechanism is chemisorption and the adsorption procedure follows the pseudo second order model [43].

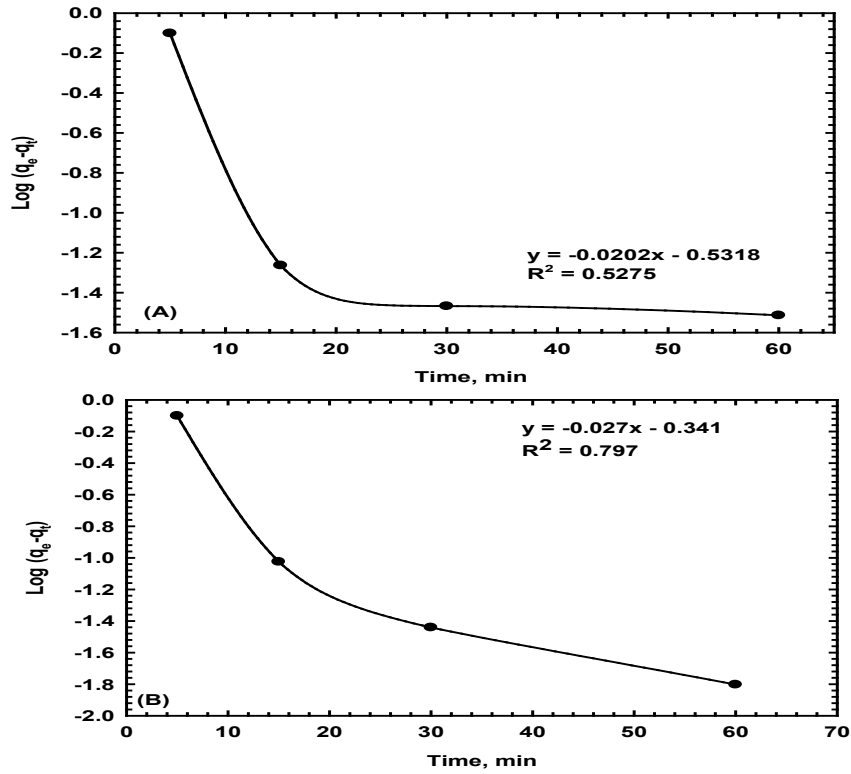


Fig. 9. Pseudo first-order kinetic model for (A)  $\text{Ni}^{+2}$ (B)  $\text{Cu}^{+2}$  ionson zeolite.

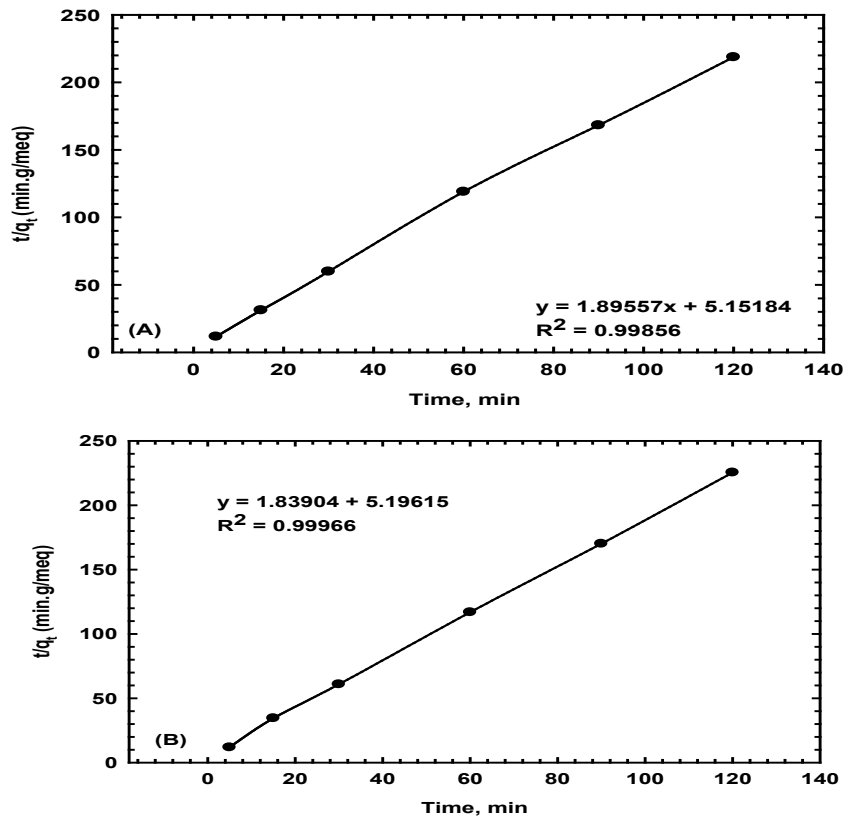


Fig. 10. Pseudo second-order kinetic model for(A)  $\text{Ni}^{+2}$ (B)  $\text{Cu}^{+2}$  ions on zeolite.

### Corrosion results for synthetic wastewater

#### Open circuit potential

Figure 12 spectacles the influence of contact time on the open or free corrosion potential (OCP) of steel probe through elapsed period of about 30 min in untreated and treated wastewater and in existence of 20 ppm  $\text{Cu}^{+2}$  and/or  $\text{Ni}^{+2}$ . The discrepancy of OCP have the same trends, since the OCP values are speedily shifted towards more negative direction in the early stage of immersion until nearly steady state conditions is reached., The OCP of the treated and the untreated wastewater was almost the same along the 30 min of immersion. The steady potential is indorsed to the creation of ferrous oxide at the probe superficial as a result of the interface between the surrounding media and the electrode surface, which prevent and protect its surface from extra attack [44]. Presence of heavy metal cations,  $\text{Cu}^{+2}$  and  $\text{Ni}^{+2}$ , in the test solution shifts the overall potential to more positive values. The positive shift caused by  $\text{Ni}^{+2}$  is much higher than that related to  $\text{Cu}^{+2}$ . The improvement of the OCP by both  $\text{Cu}^{+2}$  and  $\text{Ni}^{+2}$  could

be related to the incorporation of  $\text{CuO}$ ,  $\text{NiO}$ ,  $\text{Cu}(\text{OH})_2$  and  $\text{Ni}(\text{OH})_2$  in the formed surface film rendering the film more protective. It was reported that reduction of dissolved copper (500 ppm) on steel surface could lead to formation of copper islands and enhance galvanic corrosion [45]. In contrast the results of present work showed slight improvement of corrosion behavior in presence of dissolved copper. An explanation for this could be related to the low concentration of copper (20 ppm) which was not enough to form copper islands and produce galvanic corrosion.

#### Potentiodynamic polarization measurements

Figure 13 illustrates the scanned potentiodynamic curves of steel after OCP stability time of 30 min in untreated, treated wastewater and in presence of 20 ppm from both cations. As seen in Fig. 13, the corrosion potential  $E_{corr}$  and the current density  $i_{corr}$  are all evaluated and established in Table 6. As mentioned the values of  $E_{corr}$  and  $i_{corr}$  are nearly similar for untreated and treated wastewater. In manifestation of cations, the

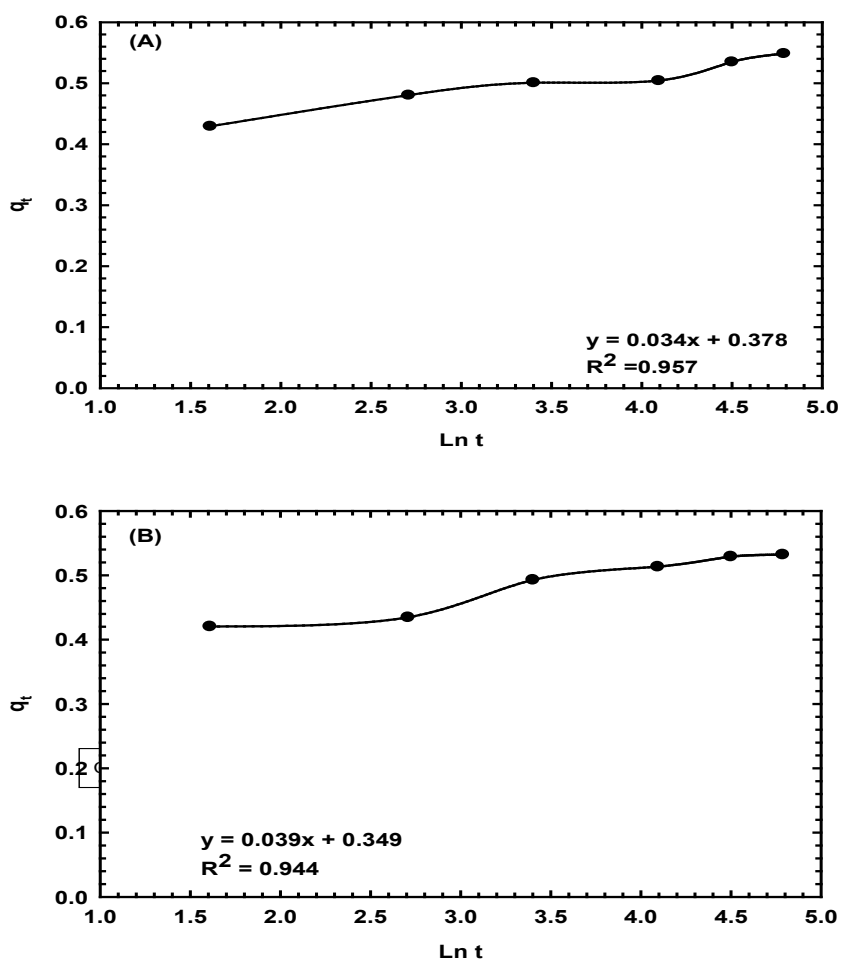


Fig. 11. Elovich kinetic model for adsorption of (A)  $\text{Ni}^{+2}$ (B)  $\text{Cu}^{+2}$  ions on zeolite at the optimum conditions.

current values are reduced and the corrosion potentials are shifted to more positive values. From the figure, it is clearly notable that, the cations had effect only on the comprehensive characteristics of the anodic lopes suggesting presence of a moderately protective film on the steel surface [46]. From the corrosion measurements,

it could be established that, the corrosion resistance of steel for treated and untreated water is almost the same. However, presence of  $\text{Cu}^{+2}$  or  $\text{Ni}^{+2}$  improved the corrosion resistance. The role of  $\text{Ni}^{+2}$  in enhancing steel surface film protectivity is higher than that of  $\text{Cu}^{+2}$ .

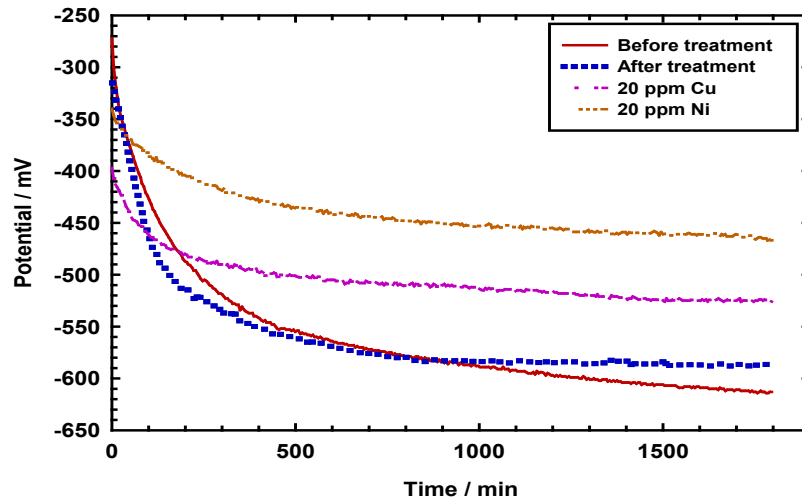


Fig. 12. Variation with time of the OCP for mild steel before and after treatment and in the presence of 20 mg/L from  $\text{Ni}^{+2}$  and  $\text{Cu}^{+2}$  ions.

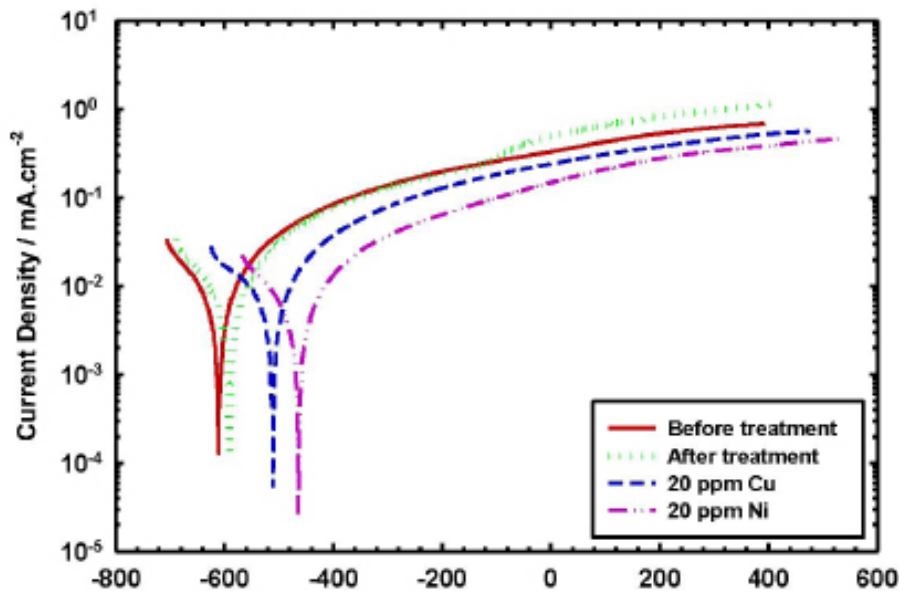


Fig. 13. Potentiodynamic polarization plots of mild steel before and after treatment and in presence of 20 mg/L from  $\text{Ni}^{+2}$  and  $\text{Cu}^{+2}$  ions at 25°C.

**TABLE 6. Electrochemical parameters and inhibition efficiency for mild steel in untreated and treated synthetic wastewater and in the presence of 20 ppm of copper and/or nickel ions.**

Synthetic wastewater	$I_{cathode}$ mA/cm <sup>2</sup>	$b_c$ mV/dec	$I_{anode}$ mA/cm <sup>2</sup>	$b_a$ mV/dec	$i_{corr}$ mA/cm <sup>2</sup>	C.R, mm/year
Before treat.	2.901	-88.00	3.607	78.39	3.254	0.0431
After treat.	2.923	-88.78	3.425	78.32	3.199	0.0424
20 ppm Cu	4.155	-87.80	1.449	60.66	2.805	0.0372
20 ppm Ni	2.508	-91.90	1.254	53.38	1.881	0.0249

### Conclusion

Zeolite was prepared from natural aluminosilicate bentonite via Zeolitization method and used as a novel effective adsorbent for adsorption of Cu(II) and Ni(II) ions from synthetic and industrial wastewater. The prepared Zeolite was characterized by XRD anal chemical analysis. The XRD results show that, zeolite contains replaceable cations such as; Na<sup>+</sup>, K<sup>+</sup>, and Ca<sup>2+</sup>. Also, the oxides Na<sub>2</sub>O and K<sub>2</sub>O were found out by flame photometry. The effect contact time, adsorbent dose and initial metal ion concentration on the adsorption performance of Cu(II) and Ni(II) ions onto zeolite was investigated through batch adsorption experiments. The kinetics and equilibrium isotherm studies proved that the adsorption process follows well the pseudo-second-order kinetic model and Freundlich isothermal models.

According to this work, the new synthesized zeolite has significant advantages in batch experimental technique. Moreover, cations can successfully get better for controlling the deterioration of steel structures. These consequences can be proved from the decreases of the deterioration rate through decreasing the values of  $i_{corr}$  and shifting of  $E_{corr}$  towards the more positive direction. The gained behavior confirms formation of a thicker and more compacted protective layer on the surface of steel structures.

### References

- Lin S. H. and Juang R. S., Heavy metal removal from water by sorption using surfactant-modified montmorillonite. *J. Hazard. Mat.*, **315**, B:92 (2002).
- Inglezakis V. J., Loizidou M. D. and Grigoropoulou H. P., Ion exchange of Pb<sup>2+</sup>, Cu<sup>2+</sup>, Fe<sup>3+</sup>, and Cr<sup>3+</sup> on natural clinoptilolite: selectivity determination and influence of acidity on metal uptake. *J. Coll. Inter. Sci.* **261**, 49-54 (2003).
- Sengupta A. K. and Clifford D., Important process variables in chromate ion exchange. *Environ Sci. Technol.* **20**, 149 (1986).
- Bailey S. E., Olin T. J., Bricka R. M. and Adrian D. D. A., review of potentially low-cost sorbents for heavy metals. *Water Res.* **33**, 2469 (1999).
- Erdem E., Karapinar N. and Donat R., The removal of heavy metal cations by natural zeolites. *J. Collo. Inter. Sci.* **280**, 309-314 (2004).
- Corbin D. R., Burgess B. F., Vega A. J. and Farelee R. D., Comparison of analytical techniques for the determination of silicon and aluminum content in zeolites. *Anal Chem.* **59**, 2722 (1987).
- Langella A., Pansini M., Cappelletti P., de Gennaro B., de Gennaro M. and Colella C., NH<sub>4</sub><sup>+</sup>, Cu<sup>2+</sup>, Zn<sup>2+</sup>, Cd<sup>2+</sup> and Pb<sup>2+</sup> exchange for Na<sup>+</sup> in a sedimentary clinoptilolite, North Sardinia, Italy. *Micropor. Mesopor. Mat.* **37**, 337 (2000).
- Caputo D. and Pepe F., Experiments and data processing of ion exchange equilibria involving Italian natural zeolites: A review. *Micropor. Mesopor. Mat.* **105**, 222-231 (2007).
- Wang S. and Peng Y., Natural zeolites as effective adsorbents in water and wastewater treatment. *Chem. Eng. J.* **156**, 11-24 (2010).
- Badillo-Almaraz V., Trocellier P., Davila-Rangel I., Adsorption of aqueous Zn (II) species on synthetic zeolites, *Nucl. Instrum. Methods Phys Res.*; **424**, B 210SS (2003).
- Barer R. M., *Zeolites and Clay Minerals as Sorbent and Molecular Sieves*. Academic Press; New York (1987).
- Breck D. W. Crystalline molecular sieves. *J. Chem. Edu.* **41**, 678-689 (1964).
- Wang, Q., Chang, X., Li, D., Hu, Z., Li, R. and He, Q., Adsorption of chromium (III), mercury (II) and lead (II) ions onto 4-aminoantipyrine immobilized bentonite. *J. Haz. Mat.* **186**, 1076-1081 (2011).
- Randeloviæ, M., Purenoviæ, M., Zarubica, A., Purenoviæ, J., Matoviæ, B. and Momèiloviæ, M., Synthesis of composite by application of mixed

- Fe, Mg (hydr) oxides coatings onto bentonite a use for the removal of Pb (II) from water. *J Haz Mat.* **199-200**, 367-374 (2012).
15. El-Shamy A. M., Hanaa A. El-Boraey and El-Awdan H. F., Chemical Treatment of Petroleum Wastewater and its Effect on the Corrosion Behavior of Steel Pipelines in Sewage Networks. *Journal of Chemical Engineering & Process Technology*; **8**, (1-1000324), 9 (2017).
  16. El-Shamy A. M., T. Y. Soror, H. A. El-Dahan, E. A. Ghazy, and A. F. Eweas., Microbial corrosion inhibition of mild steel in salty water environment. *Mat. Chem. Phys.*; **114**, 156-159 (2009).
  17. Kul, A. R. and Koyuncu, H., Adsorption of Pb (II) ions from aqueous solution by native and activated bentonite: kinetic, equilibrium and thermodynamic study. *J of Hazard Mat.* **179**, 332-339 (2010).
  18. APHA (American Public Health Association), AWWA (American Water Works Association), and WEF (Water Environment Federation), *Standard Methods for the Examination of Water and Wastewater*, 22nd edn., edited by E. W. Rice, R. B. Baird, A. D. Eaton, L. S. Clesceri, Washington, DC (2012).
  19. Shi Z., Liu M. and Atrens A., Measurement of the corrosion rate of magnesium alloys using Tafel extrapolation. *Corr. Sci.*; **52**, 579-588 (2010).
  20. Gao H., Li Q., Chen F. N., Dai Y., Luo F., Li L. Q. Study of the corrosion inhibition effect of sodium silicate on AZ91D magnesium alloy. *Corr. Sci.*; **53**, 1401-1407 (2011).
  21. Faghihian H. and Godazandeha N., Synthesis of nano crystalline zeolite Y from bentonite. *J Porous Mater.* **16**, 331-335 (2009).
  22. Galli E., Gottardi G., Mayer H., Preisinger A. and Passaglia E. The structure of potassium-exchanged heulandite at 293, 373 and 593 K. *Acta. Crystallogr Sect.*; **189**, B 39 (1983).
  23. Chisholm, Hugh, ed. Chabazite, *Encyclopædia Britannica*. **5** (11<sup>th</sup>ed), Cambridge University Press; 785 (1911).
  24. Maksin D.D., Kljajević S.O., Đolić M.B., Marković J.P., Ekmešević B.M., A.E. Onjia and Nastasović A.B., Kinetic modeling of heavy metal sorption by vinyl pyridine based copolymer, *Hem. Ind.* **66**, 795-804 (2012).
  25. Raj K Vays, Shashi and Surendra Kumar, Determination of micropore volume and surface area of zeolite molecular sieves by D-R and D-A equations: a comparative study. *Indian Journal of Chemical Technology*, **11**, 704-709 (2004).
  26. Rengaraj S. Joo C. and Kim Y., Kinetics of removal of chromium from water and electronic process wastewater by ion exchange resins: 1200H, 1500H and IRN97H J. Yi. *J. Hazard. Mater.* **102**, 257-275 (2003).
  27. Wu D., Sui Y., He S., Wang X., Li C. and Kong H., Removal of trivalent chromium from aqueous solution by zeolite synthesized from coal fly ash. *J Hazard Mat.* **155**, 415-423 (2008).
  28. Cabrera C., Gabaldón C. and Marzal P., Sorption characteristics of heavy metal ions by a natural zeolite. *J Chem. Technol. Biotechnol.* **80**, 477-481 (2005).
  29. Peri J. C., Trgo M. and Medvidovic N. V., Removal of zinc, copper and lead by natural zeolite – a comparison of adsorption isotherms. *Water Res.* **38**, 1893-1899 (2004).
  30. Mondale K. D., Carland R. M. and Aplan F. F., The comparative ion exchange capacities of natural sedimentary and synthetic zeolites. *Miner Eng.* **8**, 535-548 (1995).
  31. Langmuir I., The adsorption of gases on plane surfaces of glass, mica and platinum. *J. Am. Chem. Soc.* **40**, 1361 (1918).
  32. Hasany S. M., Saeed M. M. and Ahmed M. Sorption and thermodynamic behavior of zinc (II)-thiocyanate complexes onto polyurethane foam from acidic solutions, *J. Radioanal. Nucl. Chem.* **252**, 477 (2002).
  33. Helfferich F., *Ion Exchange*, Mc Graw-Hill New York (1962).
  34. Khan S. A., Rehman U. R. and Khan M. A. Adsorption of chromium (III), chromium (VI) and silver (I) on bentonite. *Waste Manage*; **15**, 271 (1995).
  35. Rieman W. and Walton H. Ion Exchange in Analytical Chemistry, in: *International Series of Monographs in Analytical Chemistry*; **38**, Pergamon Oxford (1970).
  36. Özcan A. S. and Özcan A., Adsorption of acid dyes from aqueous solutions onto acid-activated bentonite. *J. Colloid Interface Sci.* **276**, 39-46 (2004).
  37. Jama M. A. and Yücel H. Equilibrium studies of sodium ammonium, potassium ammonium, and calcium ammonium exchanges on clinoptilolite zeolite. *Sep Sci. Technol.*; **24** (15), 1393 (1990).
  38. Saygideger S., Gulnaz O., Istifli E.S. and Yucel N., Adsorption of Cd(II), Cu(II) and Ni(II) ions by Lemna minor L.: effect of physicochemical environment. *J. Hazard. Mater.* **126**, 96-104 (2005).
  39. Su-Hsia L. and Ruey-Shin J., Adsorption of phenol and its derivatives from water using synthetic resins and low-cost natural adsorbents: A review. *Egypt. J. Chem.* **62**, No. 9 (2019)

- J. Environ. Manage.* **90**, 1336–1349 (2009).
40. Chien S. H. and Clayton W. R. Application of Elovich equation to the kinetics of phosphate release and sorption on soils. *Soil Sci. Soc. Am. J.*; **44**, 265-268 (1980).
41. Unuabonah E.I., Adebowale K.O., Olu-Owolabi B.I., Yang L.Z. and Kong L.X., Adsorption of Pb (II) and Cd (II) from aqueous solutions onto sodium tetraborate modified kaolinite clay: Equilibrium and thermodynamic studies. *Hydrometallurgy*, **93**, 1–9 (2008).
42. Perez-Marin A. B., Meseguer V., Zapata, Ortuno J. F., Aguilar M., Sases J. and Llorens M., Removal of cadmium from aqueous solutions by adsorption onto orange waste. *J Hazard Mat B.* **139**, 122-131 (2007).
43. Qiufa Xu, Kewei Gao, Wenting Lv, Xiaolu Pang. Effects of alloyed Cr and Cu on the corrosion behavior of low-alloy steel in a simulated groundwater solution. *Corrosion*. **102**, 11-124 (2016).
44. Yoon-Seok Choi, Jae-Joo Shim, Jung-Gu Kim. Effects of Cr, Cu, Ni and Ca on the corrosion behavior of low carbon steel in synthetic tap water. *Journal of Alloys and Compounds*, **391**, 162-169 (2005).
45. Kuntal Sarkar Avik, Mondal Anindita, Chakraborty Mohit Sanbui, Nitu Rani and Monojit Dutta Investigation of microstructure and corrosion behaviour of prior nickel deposited galvanised steels. *Surface and Coatings Technology*. **348**, 64-72 (2018).

### الحد من تأثير أيونات النحاس الثنائية والنيكل الثنائية من المياه الملوثة باستخدام الممتزات المتوسطة المسامية: تأثير معالجة المياه الملوثة على سلوك التآكل لأنابيب الصلب

محمد فاروق شحاتة<sup>١</sup>، شيماء السيد الشافعي<sup>٢</sup>، نبيلة صالح عمار<sup>٣</sup> و أشرف الشامي<sup>١</sup>  
<sup>١</sup>معمل الكيمياء الكهربية - قسم الكيمياء الفيزيائية - المركز القومي للبحوث - الجيزة - مصر.  
<sup>٢</sup>معمل كيمياء السطوح والحفز - قسم الكيمياء الفيزيائية - المركز القومي للبحوث - الجيزة - مصر.  
<sup>٣</sup>معمل بحوث تلوث المياه - قسم تلوث المياه - المركز القومي للبحوث - الجيزة - مصر.

من المعروف أن عمليات تشطيب المعادن والطلاء الكهربائي ينتج عنها كميات كبيرة من المخلفات السائلة الملوثة للمياه بالمعادن الثقيلة. وفي هذه الدراسة تم تحضير زيوليت ذو مسامية متوسطة من البنتونيت المصري باستخدام طريقة الهيدروثرمل في وجود هيدروكسيد الصوديوم. ولقد تم إجراء توصيف مورفولوجي وبللوري ومسامي لعينة الزيوليت المحضرة باستخدام الميكروسكوب الماسح الإلكتروني حيود الأشعة السينية والتي تبين منها تشكيل أطوار بللورية تتوافق مع بنية الزيوليت وطيف الأشعة السينية المشتتة للطاقة. لقد تمت هذه الدراسة على مرحلتين. المرحلة الأولى اهتمت بدراسة مفصلة لأداء الزيوليت نحو امتزاز وإزالة أيونات النيكل والنحاس الثنائية عن طريق تطبيق المعادلات الرياضية ودراسة العوامل المؤثرة على التجارب العملية. حيث تم دراسة عدة عوامل منها عامل الزمن وجرعة المادة الماصة والتركيز الأولي لأيونات النحاس والنيكل في المحلول. وقد تم إجراء تجارب الإمتصاص لعمل الدراسات الحركية بهدف تعيين آلية الإمتزاز من خلال تطبيق المعادلات ذات الرتبة الأولى وذات الرتبة الثانية وفي النهاية تم حساب المعاملات الحرارية وإفترض الميكانيكية المناسبة لعملية الإمتزاز. وأظهرت نتائج نماذج الحركة أن عملية امتزاز الزيوليت لأيونات النحاس والنيكل كانت مرضية بعد 90 دقيقة وإنها تتبع الدرجة الثانية الكاذبة وأنها مناسبة جدا مع أيزوثرم لانجمير. ولقد كانت الطاقة الحرة المنطلقة من عملية الإمتزاز لكل من أيونات النحاس والنيكل هي 10.66 و 8.77 كجول/مول مما يؤكد أن عملية الإمتزاز عملية ماصة للحرارة. ثم انتقلت الدراسة للمرحلة الثانية وفي هذه المرحلة تم دراسة تأثير معالجة المياه الملوثة على السلوك التآكل لخطوط الأنابيب الفولاذية. وقد أظهرت النتائج أن مقاومة التآكل للصلب للمياه المعالجة هي نفسها للمياه غير المعالجة.